Meat Science 221 (2025) 109713

Contents lists available at ScienceDirect

Meat Science

journal homepage: www.elsevier.com/locate/meatsci

MarblingPredictor: A software to analyze the quality of dry-cured ham slices

Eva Cernadas [a,*], Manuel Fernández-Delgado [a], Manisha Sirsat [b], Elena Fulladosa [c], Israel Muñoz [c]

[a] Centro Singular de Investigacion en Tecnoloxias Intelixentes da USC (CiTIUS), Universidade de Santiago de Compostela, R/Xenaro de la Fuente Dominguez, Santiago de Compostela 15782, Spain
[b] Departamento de Gestao de Dados e Analise de Risco, Innov Plant Protect, Estrada de Gil Alvaz, Apartado 72, Elvas 7350-478, Portugal
[c] Institute of Agrifood Research and Technology (IRTA), Food Technology, Finca Camps i Armet, Girona 17121, Spain

ARTICLE INFO

Keywords:
Dry-cured ham
Intramuscular fat
Marbling
Support vector regression
Texture analysis
Image segmentation
Subcutaneous fat

ABSTRACT

Dry-cured ham is a traditional Mediterranean meat product consumed throughout the world. This product is very variable in terms of composition and consumer's acceptability is influenced by different factors, among others, visual intramuscular fat and its distribution across the slice, also known as marbling. On-line inter and intramuscular fat evaluation and marbling assessment is of interest for classification purposes at the industry. Currently, this assessment can only be performed by visual inspection and traditional sensory panels. The current work presents the software MarblingPredictor, which predicts the marbling score of the three most representative ham muscles from square regions of interest automatically extracted from a ham slice. It also estimates the rate of subcutaneous and intermuscular fat content in the ham slice. Using MarblingPredictor, the mean absolute error between the true and predicted marbling scores was 0.53, very similar to the error of sensory panellist, which is 0.50. The correlation between the computer and sensory scores is 0.68, which means a moderate to good recognition. This result underscores the relevance of this tool for its application in the ham industry for quality control and categorization purposes.

As part of this work, we also present the dataset HamMarbling of annotated ham slices used to train and test the software with the marbling scores provided by the panellists. The MarblingPredictor software and images are available from https://citius.usc.es/transferencia/software/marblingpredictor for Windows- and Linux-based systems for research purposes.

1. Introduction

Dry-cured ham is a highly appreciated and traditional product elaborated in many countries, especially in the Mediterranean basin, that enjoys a great popularity among consumers around the world. Flavour and texture are some of the most appreciated characteristics by consumers. The product quality is affected by many factors, such as the processing conditions, fat content and specially its fat distribution. Since dry-cured ham is usually consumed in sliced format, consumer's acceptability is influenced by the appearance of the slices such as subcutaneous fat and/or color, and in particular, by the intramuscular fat (IMF) and the distribution of this fat, also known as marbling (Cernadas, Durán, & Antequera, 2002). Automatic classification of slices according to the marbling degree, as well as detection of steatosis (areas with excessive intramuscular fat) and excessive intramuscular/subcutaneous fat, is of interest for the industry, as this will allow producers to improve quality controls.

Nowadays, different sensory evaluation scales are used for classifying meat products according to their marbling degree e.g., National Pork Producers standards (Moines, 1999). These scales are used by panels of trained experts to evaluate meat products. For dry-cured ham, a marbling evaluation scale has been recently designed.[1] However, these methods are not feasible for the daily control at the industry because they are tedious and very time-consuming.

* Corresponding author.
E-mail addresses: eva.cernadas@usc.es (E. Cernadas), manuel.fernandez.delgado@usc.es (M. Fernández-Delgado), elena.fulladosa@irta.cat (E. Fulladosa), israel.munoz@irta.cat (I. Muñoz).

[1] https://www.irta.cat/wp-content/uploads/2022/06/Manual-de-evaluacion-sensorial-de-jamon-y-paleta-curados_31052022.pdf

https://doi.org/10.1016/j.meatsci.2024.109713
Received 19 April 2024; Received in revised form 29 October 2024; Accepted 16 November 2024
Available online 28 November 2024

In the latest years, many approaches based on digital image analysis have been proposed for food quality assesment (Meenu et al., 2021; Pu, Yu, Sun, Wei, & Wang, 2023), like for the potatoes (Sanchez, Hashim, Shamsudin, & Mohd Nor, 2020), fruit damage (Mahanti et al., 2022), or even ham (Valous, Mendoza, & Sun, 2010). In the field of meat products, researchers applied computer image analysis to evaluate the segmentation and distribution of IMF in different meat products. These technologies are, generally speaking, non-invasive and easily replicable. Moreover, their implementation costs have decreased considerably. Different image analysis methods have been applied to segment IMF in different meat products, including beef Longissimus dorsi muscle (Jackman, Sun, & Allen, 2009; Kucha, Liu, Ngadi, & Gariépy, 2023; Liu, Sun, Young, Bachmeier, & Newman, 2018; Uttaro, Zawadski, Larsen, & Juárez, 2021) in pork loin or dry-cured ham (Ávila et al., 2019; Cernadas et al., 2002; Cernadas, Carrión, Rodríguez, Muriel, & Antequera, 2005; Muñoz, Gou, & Fulladosa, 2019; Santos-Garcés, Muñoz, Gou, Garcia-Gil, & Fulladosa, 2014). Evaluation of IMF distribution or marbling has also been studied for differente meat products such as longissimus muscle of pigs (Faucitano, Rivest, Daigle, Lévesque, & Gariepy, 2004, pork meat (Huang, Liu, Ngadi, & Gariépy, 2013; Liu, Ngadi, Prasher, & Gariépy, 2012) and dry-cured ham (Cernadas, Fernández-Delgado, Fulladosa, & Muñoz, 2022; Muñoz, Rubio-Celorio, Garcia-Gil, Guàrdia, & Fulladosa, 2015; Velásquez, Cruz-Tirado, Siche, & Quevedo, 2017).

The performances of these computer vision techniques are quite satisfactory for IMF detection and marbling evaluation. However, there are several challenges that needs to be addressed. For instance, the degree of marbling of slices not only varies among different ham pieces, but also within the same ham and within the muscles in the same slice. Moreover, the color of the fat tissues may vary considerably from one ham to another, making difficult to segment correctly the fat tissue. Differences in color are usually associated with different degrees of drying. Whereas subcutaneous fat can be relatively easy to segment, because of its location near the border in the slice, IMF may be trickier as in many cases consists of small streaks with a wide range of white tonalities, being difficult to detect. This can become even harder due to the presence of precipitates (phosphates of tyrosine crystals) with a color similar to some fat specks.

This paper presents MarblingPredictor, a software tool that can be used to segment subcutaneous and intermuscular fat from images of sliced dry-cured ham, and at the same time to predict the marbling scores in different muscles applying pretrained regression models based on image texture analysis. The tool allows to re-train these models in order to fit new available data. This software can be used in research studies or to design vision systems for the in-line classification of meat products in industry.

2. Methods

MarblingPredictor is a multi-platform (Windows and Linux) desktop application developed in C++ using the GTK+ and the OpenCV libraries for the development of graphical user interface and automatic image processing, respectively. This software automatically predicts the marbling of the three most important muscles present in a ham slice, *Biceps Femoris* (BF), *Semimembranosus* (SM) and *Semitendinosus* (ST). Besides, it recognizes the area of the subcutaneous fat and intermuscular fat. Fig. 2 shows a screenshot of MarblingPredictor with a typical image of ham slice loaded and the lateral (right) panel displayed. Subsection 2.1 describe the adquisition system of ham samples. The architecture and main funcionality of MarblingPredictor is described in subsection 2.2, while subsections 2.3 and 2.4 explain the algorithms included in the software to detect the muscles and fat, and to predict the marbling score, respectively.

2.1. Materials

The image acquisition system of ham slices was described in our previous work (Cernadas et al., 2022). It is composed of a calibrated digital camera Canon EOS 50D and an objective Canon EF-S 18–200 mm f/3.5–5.6 IS.

For each slice, sensory analysis (marbling evaluation) was carried out by three trained panellists (ISO 8586-2: 2012) and consisted of a visual assessment of the marbling of Biceps femoris (BF), Semimembranosus (SM) and Semintendinosus (ST) muscles present in the dry-cured ham slice, independently (Arboix, Boadas, Gou, & Valero, 2000; Arnau, Guerrero, Casademont, & Gou, 1995). Fig. 1 shows examples of these muscles on the ham slice image. Marbling was scored by consensus by means of scoring scale from 0.5 (minimum marbling) to 10 (maximum marbling) at intervals of 0.5 using a previously defined marbling sensory scale.[2] The marbling evaluation was done in triplicate by the panellists, achieving a standard deviation among trials of 0.5 points. This deviation was estimated from the scores of a set of slices that were evaluated by panellists at different days.

Commercial dry-cured hams were used in the experiments coming from different ham producers, corresponding to crosses from different pig breeds and having a wide range of marbling, from 0.5 to 9. See also (Cernadas et al., 2022) for a detailed description for the process to obtain the ham slices. The image dataset is composed of 741 images corresponding to different muscles extracted from each side of 371 dry-cured ham slices (one slice per ham). Specifically, 351 for BF, 335 for SM and 55 for ST.

2.2. Functionality of MarblingPredictor

MarblingPredictor manages three types of files: 1) image files to store the image; 2) XML (eXtensible Markup Language) files to save the objects with the analysis of the image; and 3) CSV (comma-separated values) files to export analysis measures and marbling scores. It is structured in three layers: the graphical modules for user interaction, the application modules to process the images and predict the marbling score, and the persistence modules to save the XML and CSV files. Fig. 3 shows the flowchart with the main tasks of MarblingPredictor. After opening a slice image, MarblingPredictor extracts the regions of interest recognizing automatically the ham slice outline, subcutaneous and intermuscular fat, and three square regions (see Fig. 2) representing the most representative ham muscles (BF, SM and ST). The marbling score for each muscle and the percentage of occupied area by subcutaneous and intermuscular fat are visualized, and can be saved into XML and CSV files. Using the edition tools, the visible objects can be moved, deleted or modified. The user can also add new fat regions or muscles with irregular shapes, and all results (marbling scores and fat percentage) can be recalculated. Anytime, the user can set the working preferences, train the regression model or export joined results of various ham slices. A detailed description of the MarblingPredictor functionality can be found in the user guide, provided as supplementary material.

2.3. Recognition of muscles and fat in the ham slice

The visible muscles in ham slices are irregular regions (see Fig. 1). But, MarblingPredictor only recognizes automatically square regions of interest (ROIs) of size *s* pixels inside the three most representative ham muscles to predict their marbling scores. The ROI size *s* can be set by the user in the MarblingPredictor preferences, and its value depends on the spatial resolution used to acquire the images. The main steps to automatically analyze an image of ham slice using MarblingPredictor are: 1) extract the outline of ham slice; 2) extract the contour of the hole in the ham slice, if present– this hole corresponds to the bone of the pig leg–; 3) recognize the contours of the subcutaneous fat; 4) recognize the contours of the intermuscular fat; 5) extract the square ROIs of size *s* for

[2] https://www.irta.cat/wp-content/uploads/2022/06/Manual-de-evaluacion-sensorial-de-jamon-y-paleta-curados_31052022.pdf

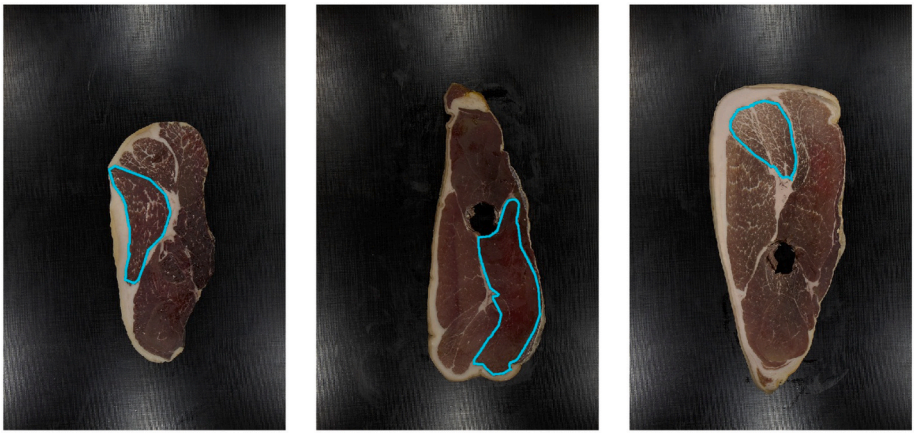

Fig. 1. Examples of ham slice images where the most representative muscles in the ham are surrounded by a blue line. (For interpretation of the references to color in this figure legend, the reader is referred to the web version of this article.)

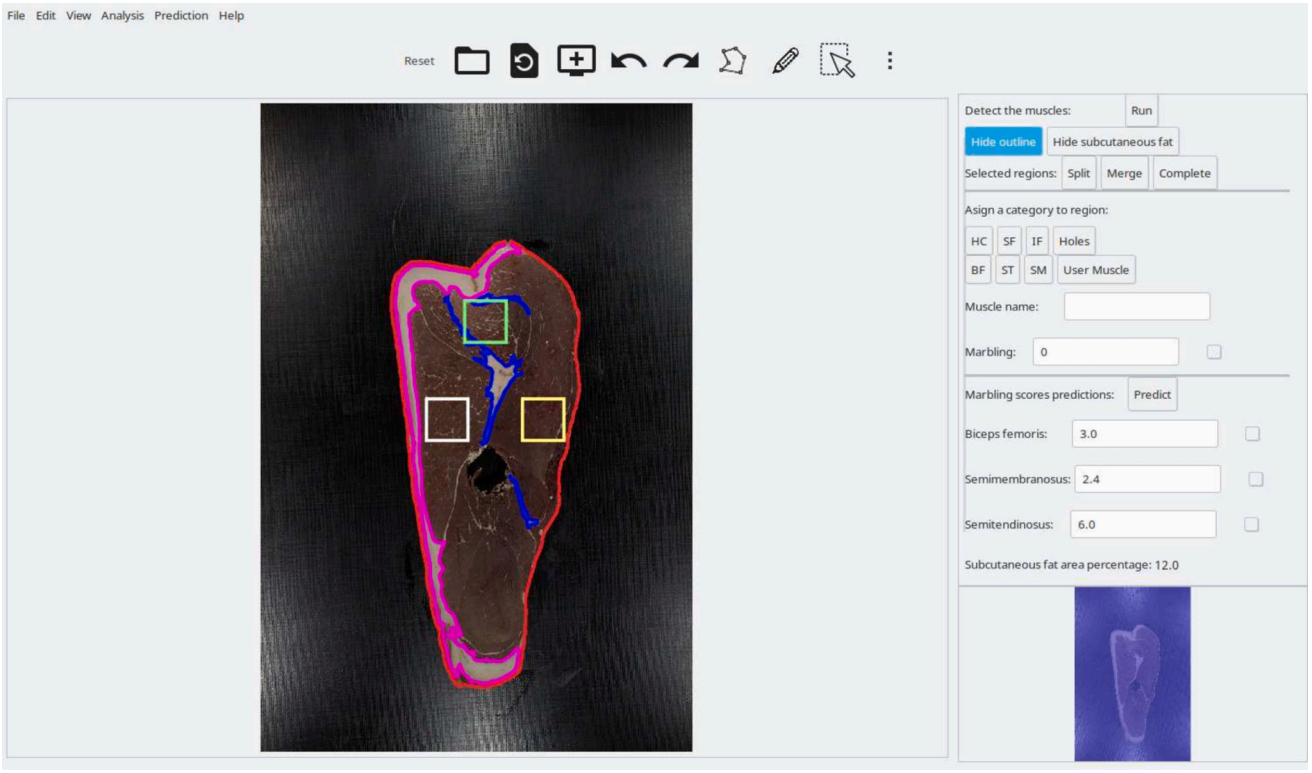

Fig. 2. Screenshot of the software MarblingPredictor. The color of the overlays (left panel) shows the type of structure: red for slice outline, pink to subcutaneous fat and dark blue to intermuscular fat. The white, yellow and green squares represent respectively the region of interest automatically extracted for the *biceps femoris*, *semimembranosus* and *semitendinosus* muscles. (For interpretation of the references to color in this figure legend, the reader is referred to the web version of this article.)

each muscle BF, SM and ST; and 6) predict the marbling score of some region in the ham slice, automatically detected in step 5 or drawn manually by the user (see subsection 2.4 for the description). The algorithm to extract the square ROIs, named ExtractSquaredROI, was already proposed and validated in our previous work (Cernadas et al., 2022). Now, we present a method to recognize the muscles and fat in the image, named SegmentHamImage, whose pseudo-code is listed in algorithm 1.

Although the acquisition systems provide images in the RGB color space, we use the Lab color space in some steps of the image processing due to its better behaviour with differences in the illumination. Let $I(x,y)$, $x = 1,\ldots,N$ and $y = 1,\ldots,M$ be the original RGB image of the ham slice, and let I_b be the b channel of the Lab image processed by a median filter with a mask of 5 pixels in order to attenuate random noise (see an example in the I_b image in Fig. 4). Most of the I_b image is the area outside the ham slice, which is almost constant. So, the maximum grey level of the histogram H_b of I_b is calculated, and it is used to create a binary image B from I_b using the criterion: $B(x,y) = 0$ if $|I_b(x,y) - H_b| \leq$ *offset* and $B(x,y) = 1$ otherwise. An offset of 5 grey levels is used in order to avoid spurious noise. The B image is post-processed with morphological open and close filters using a masksize of 5 pixels, I_{Bb}, in order to remove small black or white regions in the image. Afterwards, the

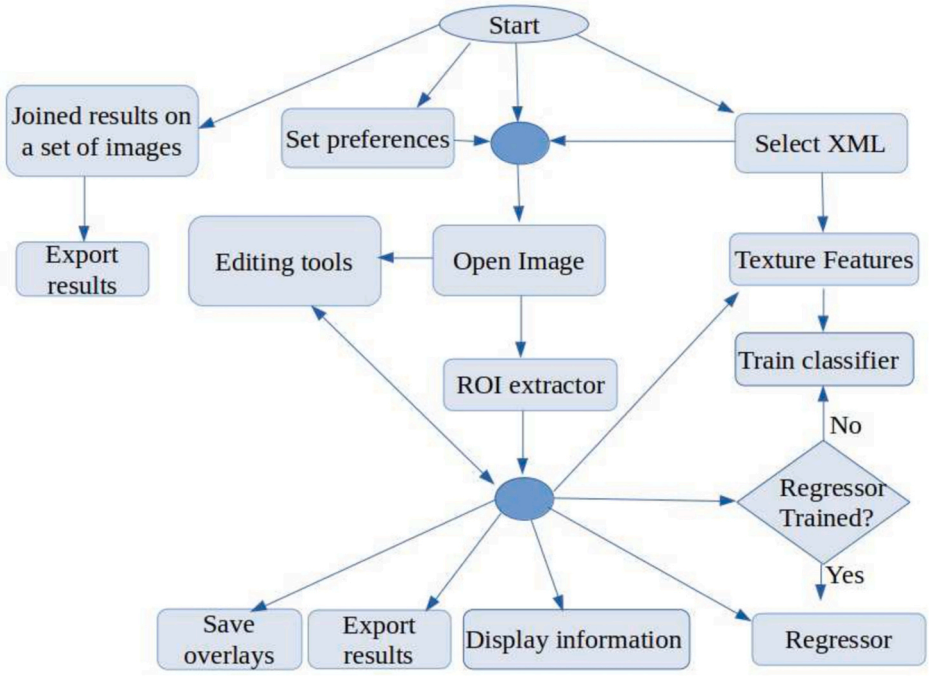

Fig. 3. The flowchart with the main tasks of MarblingPredictor.

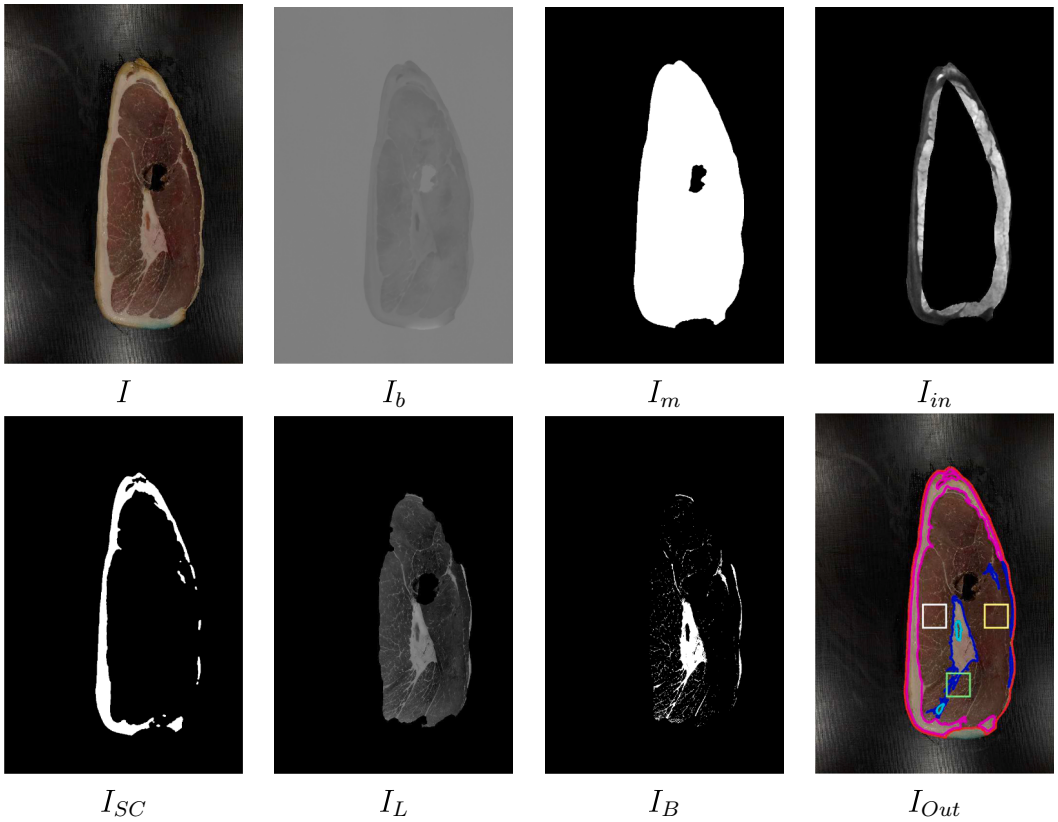

Fig. 4. An example of the automatic processing of ham slice image no. 89590 using the SegmentHamImage method: I (original image), I_b (channel b of Lab image of I after processing by a median filter, I_m (mask image with the ham slice in white), I_{in} (absolute value of b minus a channels of Lab image masked by a eroded version of I_m), I_{SC} (subcutaneous fat in white), I_L (L channel of Lab image without subcutaneous fat) and I_B (binarization of I_L image) (see algorithm 1 for details). The image I_{Out} shows the set of contours $\mathscr{S}$ overlapped to the original image: outline ham (red), subcutaneous fat (pink), intermuscular fat (dark blue), holes in intramuscular fat (blue) and square ROI for BF (white), SM (yellow) and ST (green) muscles. (For interpretation of the references to color in this figure legend, the reader is referred to the web version of this article.)

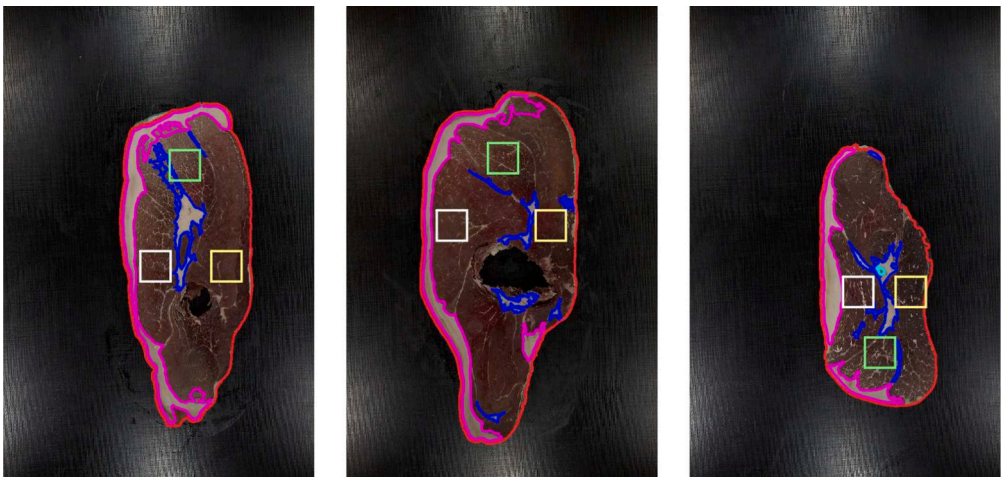

Fig. 5. Examples of the visual performance of the SegmentHamImage algorithm for several ham slices. The color means different type of objecs: ham outline (red), subcutaneous fat (pink), intermuscular fat (dark blue) and square BF (white), SM (yellow) and ST (green) muscles. (For interpretation of the references to color in this figure legend, the reader is referred to the web version of this article.)

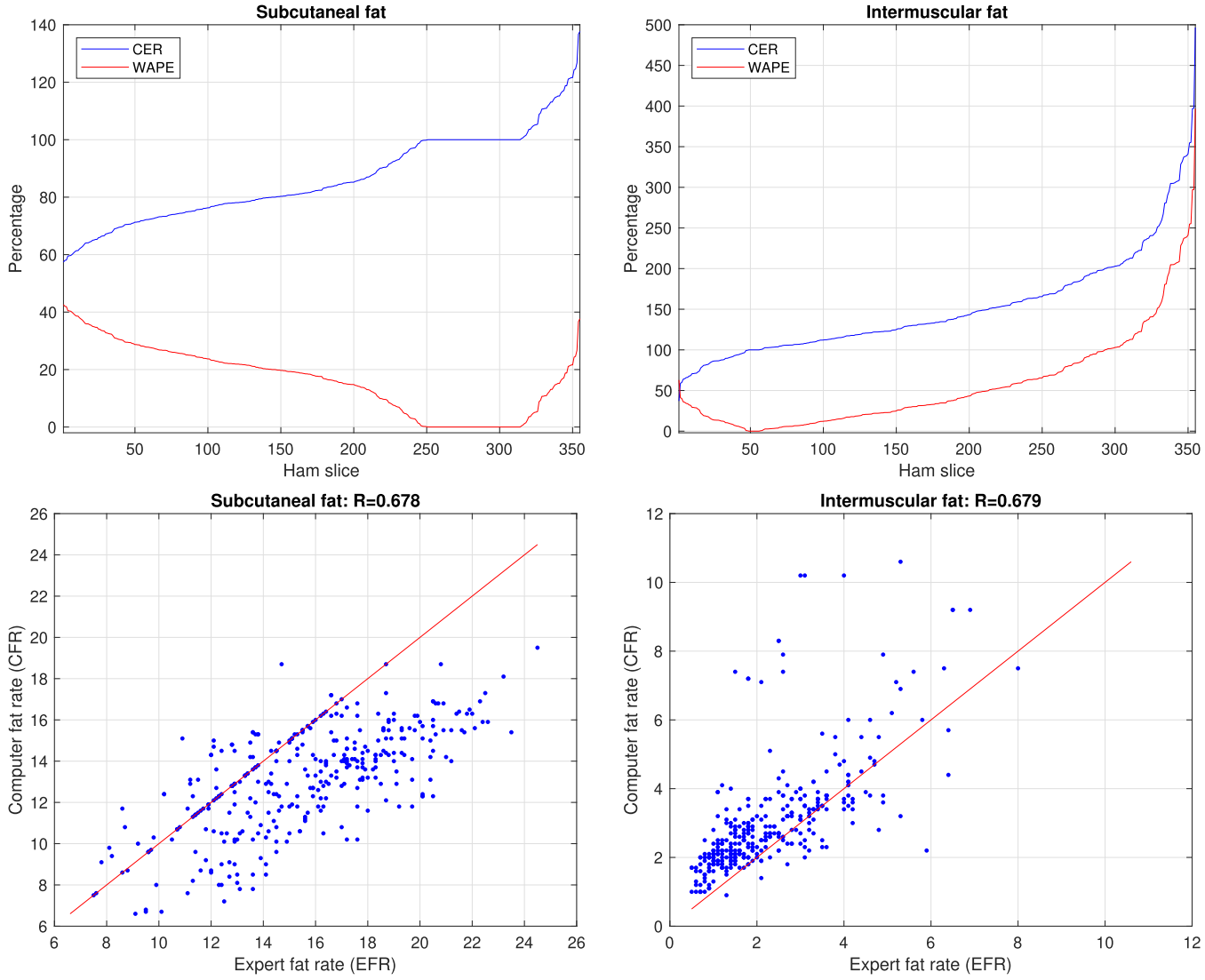

Fig. 6. Upper row: Computer Expert Rate (CER) and Weighted Absolute Percentage Error (WAPE) of fat content for each ham slice for subcutaneous fat (left panel) and intermuscular fat (right panel). Lower row: scatterplot of the expert and computer fat rate for the subcutaneous fat (left panel) and intermuscular fat (right panel). The correlation R is reported in the title.

contours of the regions in I_{Bb} image are extracted using the algorithm proposed by Suzuki and Be (1985). The ham outline c_o is extracted as the biggest external region, while the hole contour c_h, if present, is extracted as the biggest internal region with more than 1000 pixels. A mask image I_m shown in Fig. 4 is built considering the inside of c_o as white and c_h as black respectively.

Algorithm 1. Automatic segmentation of a ham slice image.

Algorithm: $\mathcal{S}$=SegmentHamImage(I, s)
Data: I: original RGB image of ham slice; s: size of ROI
Result: $\mathcal{S} = \{c_i\}_{i=1}^{N_S}$: set of regions recognized
$I_{a'}, I_{b'} \leftarrow a$ and b channel of Lab image of I
// slice outline
$I_b \leftarrow$ median filtering with mask 5 of $I_{b'}$
$H_b \leftarrow$ maximum of histogram of I_b
$B(x,y) \leftarrow 0$ if $|I(x,y) - H_b| \leq 5$ and 1 otherwise
$I_{Bb} \leftarrow$ binary image B after morphological processing
$c_o \leftarrow$ contour of the biggest external region in I_{Bb}
$c_h \leftarrow$ contour of the biggest internal region in I_{Bb}
$A_{ham} \leftarrow$ area(c_o)
$I_m \leftarrow$ mask image filling c_o with 1
// subcutaneous fat
$I_{ba} \leftarrow |I_{b'}(x,y) - I_{a'}(x,y)| \; \forall (x,y)$
$I_{in} \leftarrow I_{ba}$ masked by an eroded version of I_m
$t_1, t_2, t_3 \leftarrow$ Otsu3ThresWB(I_{in})
$T \leftarrow (t_1 + t_2)/2$
$I_{SC'} \leftarrow 1$ if $I_{in} < T$ and 0 otherwise
$I_{SC} \leftarrow I_{SC'}$ after open filtering
$\mathcal{B} \leftarrow$ external contours in I_{SC}
$\{c_i^{SC}\}_{i=1}^{N_{SC}} \leftarrow \{c_i \in \mathcal{B} |$ area$(c_i) < 0.005 A_{ham}$ and touch$(c_i, c_o)\}$
// intermuscular fat
$I_{L'} \leftarrow L$ channel of Lab image of I
$I_m^L \leftarrow I_m$ image with $\{c_i\}_{i=1}^{N_{SC}}$ filled with 0
$I_L \leftarrow I_{L'}$ multiplied by a eroded version of I_m^L
$t_1^L, t_2^L, t_3^L \leftarrow$ Otsu3ThresWB(I_L)
$I_B(x,y) \leftarrow 1$ if $I_L(x,y) > t_3^L$ and 0 otherwise
$\mathcal{C} \leftarrow$ external and internal contours in I_B
$\{c_i^{IF}\}_{i=1}^{N_{IF}} \leftarrow \{c_i \in \mathcal{C} | \; c_i$ external and area$(c_i) > 0.01 A_{ham}\}$
$\{c_i^{HF}\}_{i=1}^{N_{HF}} \leftarrow \{c_i \in \mathcal{C} | \; c_i$ internal and area$(c_i) > 0.01 A_{ham}\}$
// ExtractSquaredROI(): algorithm 1 in (Cernadas et al., 2022)
$I_{BF}, I_{SM}, I_{ST} \leftarrow$ ExtractSquaredROI(I, s)
$c_{BF}, c_{SM}, c_{ST} \leftarrow$ bounding box coordinates of I_{BF}, I_{SM}, I_{ST}
$\mathcal{S} \leftarrow \{c_o\} \cup \{c_h\} \cup \{c_i^{SC}\}_{i=1}^{N_{SC}} \cup \{c_i^{IF}\}_{i=1}^{N_{IF}} \cup \{c_i^{HF}\}_{i=1}^{N_{HF}} \cup \{c_{BF}, c_{SM}, c_{ST}\}$

The subcutaneous fat is just below the skin of the ham, so it will be seen in the ham slice image touching the ham outline. So, we only analyze the image in a ring attached to the edge of the slice. A mask image with this ring $I_{m'}$ is built from the c_o contour of the ham outline, which is eroded many times (in our case, 20 times) with masksize of 5, to built the other mask image $I_{m''}$. The xor function of both mask images is multiplied by the absolute difference between b and a channel of Lab image, I_{ab}, developing the image I_{in}. The Fig. 4 shows an example of image I_{in}, normalized to the range [0,255] for visualization purposes. In this image the darker pixels are associated to fat and the brighter pixels to lean. The selection of the optimal value to threshold the image is always a critical decision, and in the literature it is often determined by trial and error. In our approach, this optimal threshold T is automatically selected from the image characteristics using the method proposed by Otsu (1979), which selects T to minimize intra-class intensity variance while maximizing inter-class variance. We used a modified version of this method, called Otsu3ThresWB, that considers four classes and does not consider the black pixels (grey level 0). Let t_1, t_2, t_3 the intensity values provided by Otsu3ThresWB(I_{in}). The selected optimal value is $T = (t_1 + t_2)/2$. A binary image is obtained setting to 255 the grey levels $I_{in}(x,y) < T, \forall (x,y)$ and to 0 the remaining pixels. This image is processed by an open filter with masksize 5 to remove spurious noise, obtaining the image I_{SC} shown in Fig. 4, where the subcutaneous fat is visualized as white regions. The subcutaneous fat regions c_i^{SC} are the external regions of I_{SC}, whose area is biggest than the 0.5% of the area of ham slice and it is touching the ham outline (function touch in algorithm 1). Let $p_j^i = \left(x_j^i, y_j^i\right) \in c_i$ be points in the contour c_i. The function touch(c_i, c_o) returns true if $\exists p_k^o$ such that $|p_k^o - p_j^i| < 10$ and false otherwise.

The intermuscular fat is located between the muscles of the ham, normally in the center of the slice. For automatically recognize this fat, we use the intensity channel of Lab color space, the L channel. A binary mask is built from the I_m image adding the contours of the subcutaneous fat filled by 0 value, and a eroded version of this image with masksize 5 is multiplied by the L channel of slice to obtain the I_L image in Fig. 4. Let t_1^L, t_2^L, t_3^L be the threshold values obtained after applying the Otsu3ThresWB(I_L) function to I_L image. The binary image I_B containing the intermuscular fat is calculated setting $I_B(x,y) = 1$ if $I_L(x,y) > t_3^L$ and $I_B(x,y) = 0$ for the remaining pixels (x,y). The contours of external white region in I_B, whose area is biggest than 1 % of ham slice area, are associated to intermuscular fat (see the dark blue contours in the I_{Out} image of Fig. 4). The internal black regions in I_B, whose are also biggest than 1 % of slice area, are associated to lean inside areas of intermuscular fat (see the light blue in image I_{Out} of Fig. 4).

Fig. 5 shows examples of the visual performance of SegmentHamImage algorithm for various ham slices. The contours of set $\mathcal{S}$ are overlapped to the original image and their color depends of the type of object: ham outline (red), subcutaneous fat (pink), intermuscular fat (dark blue), lean inside intermuscular fat (light blue) and squares with BF (white), SM (yellow) and ST (green) muscles. It is important to emphasize that all the threshold values, T and t_3^L to binarize the I_{in} and I_L images respectively, calculated by Otsu3ThresWB function, are different for each image. In this way the differences in ham slice characteristics and acquisition conditions are embedded into the segmentation algorithm, avoiding any normalization pre-processing.

2.4. Marbling score prediction

The marbling score of the muscle is a real value between 0 and 10, so the machine learning model needed to predict this score is a regressor. Once a square ROI is automatically detected by MarblingPredictor or drawn manually by the user, the software predicts the marbling score of that region by applying a machine learning regression model on a vector of color texture features extracted from the ROI. In our previous work (Cernadas et al., 2022), we evaluated several regressors belonging to different families and various color texture feature vectors. The best trade-off between performance and speed was achieved by: 1) a feature vector composed by the mean and variance of all channels of the RGB original image I inside the region, plus the Haralick coefficients contrast, homogeneity, correlation and energy of the coo-currence matrix calculated over the distances 1, 2 and 3; and 2) the epsilon-support vector regression (SVR) with radial basis function kernel. MarblingPredictor calculates the color texture features using the OpenCV library, and uses the SVR implemented by the LibSVM library (Chang & Lin, 2011), both accessed through their C++ interfaces. Each training example contains the input vector and the true output for a ham slice. The input vector includes 18 color texture features extracted from a ROI in ham slice. The true output is the marbling score set by the expert panel for the muscle where the ROI is located. For the SVR, the regularization hyperparameter λ is tuned using values $\{2^i\}$, with i from -5 to 14 with step 2, while $\gamma = 1/2\sigma^2$, where σ is the kernel spread, is tuned with values $\{2^i\}$, being i from -15 to 0. The experimental methodology that we used was 4-fold cross validation. The training set is divided into four folds, devoting three folds for training and the remaining one for validation. In order to ensure that all folds have ham slices representative of the whole range of marbling scores, the training slices are sorted by increasing marbling score. After that, slices 1, 2, 3, 4 are added to folds 1, 2, 3 and 4

respectively. Slices 5, 6, 7 and 8 are included in folds 1, 2, 3 and 4 respectively and so on. The input vector and the output (marbling score) are standardized, i.e., transformed to have zero mean and standard deviation one over the training set. The tuning of λ and γ is performed using the grid-search method. For each combination of hyper-parameters, the SVR model is trained using the three training folds, and tested on the validation fold. This training is repeated four times, and each time the validation fold is different in order to remove eventual biasings caused by the slice splitting among folds. The combination of hyper-parameters selected is the one that minimizes the average root mean square error (RMSE), over the four validation folds. The RMSE is the squared root of the mean squared differences between the true and predicted marbling score over the validation slices. The combination of λ and γ that achieves the lowest average RMSE on the validation folds is selected to train the SVR on the whole training dataset. MarblingPredictor uses the SVR trained according the previous procedure to predict the marbling score for new slices. The trained regressor is also included with the MarblingPredictor software.

3. Results and discussion

3.1. Experimental setup

In order to statistically evaluate MarblingPredictor, the 741 ham slice images of the dataset were divided in training and test sets. The slices are sorted by marbling score and, after sorting, the data 1 is asigned to training set and data 2 to test set, data 3 to training set, and data 4 to test set, and so on. In this way, each set has aproximatly the 50 % of slices, while both include slices with marbling scores distributed over the whole range of values. The training set is used to train the default regressor (SVR) included in MarblingPredictor, and the test set to evaluate the reliability of MarblingPredictor for fat calculation and marbling prediction.

The mean absolute error (MAE) is used to evaluate the ability of MarblingPredictor to predict the marbling score of ham slices in the test set. The MAE is the average absolute difference between the predicted and true marbling value, defined by:

$$MAE = \frac{1}{N}\sum_{i=1}^{N}|y_i - o_i| \tag{1}$$

where y_i and o_i are the predicted and true values of marbling, respectively, for ham slice i and N is the number of ham slices in the test set.

The performance of the algorithm to recognize the fat content (subcutaneous and intermuscular fat) is evaluated comparing the area of the ham slice image predicted by the computer with the true one. Let A_c^i, A_e^i and A_s^i be the area of fat content provided automatically by MarblingPredictor, after one expert supervision and the area of ham slice for the image i, with $i = 1, \ldots, N$. We define the CFR (Computer Fat Rate), EFR (Expert Fat Rate) and CER (Computer Expert Rate) for each image i as:

$$CFR_i = \frac{100A_c^i}{A_s^i} \qquad EFR_i = \frac{100A_e^i}{A_s^i} \qquad CER_i = \frac{100A_c^i}{A_e^i} \tag{2}$$

We also define the WAPE (Weighted Absolute Percentage Error) as the relative error of the percentage CER normalized by A_e:

$$WAPE(\%) = 100\frac{\sum_{i=1}^{N}\left|A_c^i - A_e^i\right|}{\sum_{i=1}^{N}A_e^i} \tag{3}$$

The Pearson correlation, R, between the percentage of surface recognized by the computer as fat and true percentage of fat obtained by the panellist by manual selection is the following:

$$R = \frac{\sum_{i=1}^{N}(CFR_i - \overline{CFR})(EFR_i - \overline{EFR})}{\sqrt{\left(\sum_{i=1}^{N}(CFR_i - \overline{CFR})^2\right)\left(\sum_{i=1}^{N}(EFR_i - \overline{EFR})^2\right)}} \tag{4}$$

where CFR_i and EFR_i are the fat content percentage recognized by the computer and true fat content percentage selected manually by the panellist, respectively, for ham slice i, while $\overline{CFR}$ and $\overline{EFR}$ are the mean values of $\{CFR_i\}_{i=1}^N$ and $\{EFR_i\}_{i=1}^N$, respectively.

3.2. Fat calculation results

The accuracy of MarblingPredictor to calculate the subcutaneous fat and intermuscular fat of ham slice is measured on the test set. For that, the user loaded an image and run the automatic algorithm described in section 2.3 to recognize the subcutaneous and intermuscular fat. Then, the expert checked the automatic recognition and corrects the errors modifying, adding or deleting the recognized regions, and saved the XML file for each image. The changes made by the experts using the graphical user interface (GUI) of MarblingPredictor were registed in the XML files in order to evaluate its performance. Table 1 summarizes the minimum, maximum and average fat content provided by the computer and after expert supervision (see the eqs. 2 and 3 for the meaning of CFR, EFR, CER and WAPE). In average, the fat percentage provided by computer and experts in relation to the ham slice area (columns CFR and EFR in the table) are very similar, 15.5 % provided by the computer vs. 13.1 % by the expert for the subcutaneous fat, and 2.3 % by the computer vs. 3.1 % by the expert for the intermuscular fat.

In order to find out how works the automatic algorithm to recognize the fat content, we compare the fat area recognized automatically by MarblingPredictor to the true fat area (columns CER and WAPE in the table). The true fat area recognized by the algorithm falls into the range from CER = 57.4 % to 137 % (average 86.4 %) for the subcutaneous fat, i. e. for some ham slices the subcutaneous fat recognized is lower than the true (57.4 % of true area) and for other ones is bigger than the true (137 %). For the WAPE, the error goes from 0 % (perfect recognition) to 42.6 % with an average of 16.7 %, which is a low/moderate normalized error. For the intermuscular fat (lower part of the Table 1), the recognition error is higher than for the subcutaneous fat and its dispersion also higher. A detailed view of the recognition error is shown in Fig. 6. In the upper row it is plotted the CER and WAPE for each ham slice, sorted by increasing value of CER. For the subcutaneous fat, the WAPE is lower than 20 % for the majority of ham slices (average 16.7 %). Nevertheless, for the intermuscular fat recognition the errors are higher, mainly due to the intermuscular fat area for some images is very low and small

Table 1
Average, minimum and maximum percentages of fat content of ham slice over all images (subcutaneous fat in the upper side and intermuscular fat in the bottom one) recognized automatically by the computed (CFR column) and after expert supervision (EFR column). The column CER shows the rate of area recognized by the computer divided by the true area, and its relative rate is shown in the column WAPE.

	Related to slice		Related to true area	
	CFR	EFR	CER	WAPE
subcutaneous fat				
Avg.	15.5	13.1	86.4	16.7
Min.	7.5	6.6	57.4	0.0
Max.	24.5	19.5	137.7	42.6
Intermuscular fat				
Avg.	2.3	3.1	151.7	56.6
Min.	0.5	0.9	37.1	0.0
Max.	8.0	10.6	496.6	396.6

variations in the recognition provides high error (A_e is in the denominator in eq. 3), although this fact has little influence on the automatic calculation of intermuscular fat rate (compare CFR and EFR columns in Table 1). In fact, the graphs of the lower row of Fig. 6 show a scatterplot of the expert and computer fat rate (EFR and CFR respectively), where each blue point represents one ham slice and the red line is the perfect recognition, for subcutaneous fat (left graph) and intermuscular fat (right graph). In both cases, the majority of the blue points are quite close to the red line, meaning a good estimation of fat area rate. Hence, the correlation R (see Eq. 4) of expert and computer measures of the percentage of fat content achieves R=0.68, qualified as "moderate to good" according to the criteria of Colton (1974).

3.3. Marbling prediction results

The ability of MarblingPredictor to predict marbling score is also measured on the test set. For that, the user did the following steps for each image in the test set: 1) loaded the image; 2) run the automatic algorithm to extract the square ROI for each muscle, and the regressor to predict the marbling; 3) checked the prediction for the muscle with the sensory analysis provided by the trained panellists, set the true marbling score for that muscle and checked the box in the GUI; and 4) saved the XML file for that image in order to perform the statistical analysis. Table 2 shows the results (MAE row), globally and for each muscle, achieved analysing the mentioned XML files for the test set. The MAE row is the mean absolute error between the predicted and the true marbling; rows $T < x$ are the percentage of ham slices where the difference between the predicted and true marbling value is lower than a tolerance $T = x$. The N row is the number of test images for each muscle. The average error of the automatic marbling predicted by the computer and the panellist assessed by experts is low (MAE =0.53), considering that the average variation of the expert panellist is 0.50. According to muscle, the prediction is better for BF (MAE = 0.47) than ST (MAE = 0.64). The Residual Prediction Deviation (RPD) was calculated in the R language for Statistical Computing[3] using the RPD function of the chillR package.[4] Values of RPD above 2.5 are considered an excellent agreement between true and predicted values. In our case, the RPD achieved (1.89475) is a moderate performance.

Table 2
Mean Absolute Error (MAE) between the predicted and true value for marbling score for all ham slices (column "All") and for the muscle Biceps femoris (column BF), Semimembranosus (column SM) and Semintendinosus (column ST). N is the number of ham slices. Assuming that the marbling score is correctly predicted if it is within an interval of the true marbling score, called tolerance (T), from five to eight rows show the percentage of ham slices correctly labeled. From 11 to 13 rows show this percentage after supervise the position of the automatically extracted region of interest (ROI) for each muscle.

	All	BF	SM	ST
N	356	169	159	28
Automatic prediction				
MAE	0.53	0.47	0.58	0.64
$T < 0.5$	55.9	62.7	49.7	50.0
$T < 1$	86.2	88.7	84.3	82.1
$T < 1.5$	96.1	97.6	95.0	92.8
$T < 2$	99.2	99.4	96.8	96.4
ROI position supervised				
MAE	0.29	0.26	0.30	0.37
$T < 0.5$	91.0	94.0	89.9	78.6
$T < 1$	99.4	100	98.7	100
$T < 1.5$	100	100	100	100

[3] http://r-project.org
[4] https://cran.r-project.org/web/packages/chillR/index.html

The rows below MAE in *Automatic prediction* part of Table 2 are the percentage of right classifications of ham slice. Assuming the expert assessment error in the marbling prediction (0.50), the computer classifies correctly the 55.9 % of ham slices (from 62.7 % for *biceps femoris* to 49.7 % for *semimembranosus*). Increasing the tolerance to 1, the correct classification grow up to 86.2 % and for a tolerance of 2, all ham slice are practically correctly classified (99.2 %).

The experts performed an experiment supervising the ham slices in which the difference between predicted and true marbling is higher than 0.50 (see the rows below *ROI position supervised* in Table 2). In the supervision, the expert can only move the square representing each muscle to another position with more representative characteristics. Comparing the results before and after expert supervision (upper and lower part in Table 2), all the performance metrics improve: the MAE reduces from 0.53 to 0.29, and the slice classification raises from 55.9 % to 91 % for $T < 0.5$. Then, we can conclude that the errors in marbling prediction are mainly due to a non-suitable selection of the square ROI of the ham muscles to predict the marbling score.

We also tested the ability of MarblingPredictor to predict the marbling score of irregular regions, like the contour of a whole muscle. Although the model was trained using square ROIs, we repeated the above experiment using the most important muscles drawn by experts in the test set (examples in Fig. 1). Table 3 shows the MAE achieved by type of muscle and different tolerances, reporting results similar to Table 2 or even slightly better in some cases. For example, the MAE decreases from 0.53 to 0.5 considering all muscles together. The correct classification of ham slice increases from 55.9 % to 60.7 % using a tolerance of 0.5. In this way, the irregular shape drawn by the expert guarantees that texture features are not calculated outside the muscle. This is, probably, the reason of this gain in performance. So, MarblingPredictor can be used both for predict automatically the marbling score of the muscles BF, SM and ST or to predict the marbling score of a region in the ham slice drawn by the user.

3.4. System perception

In the subsections 3.2 and 3.3, we evaluate the performance of automatic algorithms to estimate fat and marbling score in a ham slice. In this subsection, the subjective perception of experts using the marblingPredictor tool is evaluated using the system usability scale (SUS), a 10-item questionnaire (Bangor, Kortum, & Miller, 2009; Brooke, 2013) to assess the learnability and subjective perceived usability of computer systems. The interpretation of the SUS score in a 0 to 100 scale is (Sauro, 2011): <25 indicates "the worst imaginable system"; from 25 to 39 means "the worst imaginable to poor"; from 40 to 52 is "poor to acceptable"; 53 to 73 is "acceptable to good"; 74 to 85 is "good to excellent"; and above 85 indicates "excellent to the best imaginable system". The SUS questionnaire was filled by 8 experts (technicians and researchers) in meat and ham assessment of the Institute of Agrifood Research and Technology of Catalunya, which is the minimum number of people to provide a reliable score of the software. The average SUS score was 73.44 (ranging from 62.5 to 80), which means that the user

Table 3
Analogous to Table 2, but using the irregular contour of the most representative muscles drawn by the experts.

	All	BF	SM	ST
N	356	169	159	28
MAE	0.5	0.40	0.61	0.55
Automatic prediction (%)				
$T < 0.5$	60.7	70.2	50.9	57.1
$T < 1$	87.9	94.6	81.1	85.7
$T < 1.5$	97.5	99.4	95.6	96.4
$T < 2$	99.4	100	96.2	100

perception about MarblingPredictor is “acceptable to good” but very near to “good to excellent”.

4. Conclusions and future work

This paper proposes the software MarblingPredictor, that allows to predict automatically the marbling score and to calculate the subcutaneous and intermuscular fat content of a dry-cured ham slice from its image. MarblingPredictor automatically recognizes the subcutaneous and intermuscular visible fat and extracts square ROIs from the most representative muscles in the slice: BF (*Biceps femoris*), SM (*Semimembranosus*) and ST (*Semitendinosus*). The software predicts the marbling scores for the muscles calculating color texture features on the different ROIs in the ham slice. The mean absolute error (MAE) between the true score, set by a panel of experts, and the marbling prediction, provided by MarblingPredictor, is 0.53, with small differences among muscles, ranging from 0.47 for BF to 0.64 for ST. This difference is similar to the variance among the panellists, whose scores have a deviance of 0.50. The software also calculates the percentage of area occupied by subcutaneous and intermuscular fat. The Pearson correlation between the fat content estimation made by the computer and the true one is 0.68, qualified as “moderate to good” according to the Colton criteria. The experts subjectively perceived MarblingPredictor as a “good” software tool.

The results reported by MarblingPredictor are very encouraging as the algorithms implemented in this tool can be used for developing automatic quality systems working in real-time for the meat industry. The evaluation of marbling and fat in ham slices may allow companies to provide additional information for consumers and segment markets, and to offer products tailored for consumer needs (reduced fat intake, etc). The use of these algorithms could also be extended to other meat products, such as fresh meat, etc., in which fat and marbling plays also an important role. However, some challenges lie still ahead. Sliced ham is produced in packages containing several slices and it is not feasible to analyze slice by slice.

CRediT authorship contribution statement

Eva Cernadas: Writing – review & editing, Writing – original draft, Visualization, Validation, Supervision, Software, Project administration, Methodology, Investigation, Formal analysis, Conceptualization. **Manuel Fernández-Delgado:** Writing – review & editing, Validation, Supervision, Software, Methodology, Investigation. **Manisha Sirsat:** Writing – review & editing, Validation, Methodology, Investigation, Formal analysis, Data curation. **Elena Fulladosa:** Writing – review & editing, Validation, Supervision, Resources, Project administration, Investigation, Funding acquisition, Conceptualization. **Israel Muñoz:** Writing – review & editing, Writing – original draft, Validation, Supervision, Resources, Investigation, Data curation.

Declaration of competing interest

The authors declare that they have no known competing financial interests or personal relationships that could have appeared to influence the work reported in this paper.

Acknowledgements

This work has received financial support from the Xunta de Galicia (Centro singular de investigación de Galicia, accreditation 2020–2023) and the European Union (European Regional Development Fund—ERDF), Project ED431G-2019/04. IRTA's contribution was also funded by the CCLabel project (RTI-2018- 096883-R-C41) and the CERCA programme from Generalitat de Catalunya.

Appendix A. Supplementary data

Supplementary data to this article can be found online at https://doi.org/10.1016/j.meatsci.2024.109713.

Data availability

Data will be made available on request.

References

Arboix, J. A., Boadas, C., Gou, P., & Valero, A. (2000). Changes in different zones of dry-cured ham during drying moisture and sodium chloride content. *Fleischwirtschaft International: Journal for meat production and meat processing, 81*, 45–48.
Arnau, J., Guerrero, L., Casademont, G., & Gou, P. (1995). Physical and chemical changes in different zones of normal and PSE dry cured ham during processing. *Food Chemestry, 52*, 63–69.
Ávila, M., Durán, M., Antequera, T., Caballero, D., Palacios-Pérez, T., Cernadas, E., & Fernández-Delgado, M. (2019). Magnetic resonance imaging, texture analysis and regression techniques to non-destructively predict the quality characteristics of meat pieces. *Enginering Applications of Artificial Intelligence, 82*, 110–125.
Bangor, A., Kortum, P., & Miller, J. (2009). Determining what individual SUS scores mean: Adding and adjective rating scale. *Journal Usability Studies, 4*, 114–123.
Brooke, J. (2013). SUS: A retrospective. *Journal Usability Studies, 8*, 29–40.
Cernadas, E., Carrión, P., Rodríguez, P. G., Muriel, E., & Antequera, T. (2005). Analyzing magnetic resonance images of Iberian pork loin to predict its sensorial characteristics. *Computer Vision and Image Understanding, 98*, 345–361.
Cernadas, E., Durán, M., & Antequera, T. (2002). Recognizing marbling in dry-cured Iberian ham by multiscale analysis. *Pattern Recognition Letters, 23*, 1311–1321.
Cernadas, E., Fernández-Delgado, M., Fulladosa, E., & Muñoz, I. (2022). Automatic marbling prediction of sliced dry-cured ham using image segmentation, texture analysis and regression. *Expert Systems with Applications, 206*, Article 117765.
Chang, C., & Lin, C. (2011). LIBSVM: A library for support vector machines. *ACM Transactions on Intelligent Systems and Technology, 2*(27), 1–27.
Colton, T. (1974). *Statistical in medicine*. NJ: Little Brown and Co.
Faucitano, L., Rivest, J., Daigle, J. P., Lévesque, J., & Gariepy, C. (2004). Distribution of intramuscular fat content and marbling within the longissimus muscle of pigs. *Canadian Journal of Animal Science, 84*, 57–61.
Huang, H., Liu, L., Ngadi, M., & Gariépy, C. (2013). Prediction of pork marbling scores using pattern analysis techniques. *Food Control, 31*, 224–229.
Jackman, P., Sun, D.-W., & Allen, P. (2009). Automatic segmentation of beef longissimus dorsi muscle and marbling by an adaptable algorithm. *Meat Science, 83*, 187–194.
Kucha, C. T., Liu, L., Ngadi, M., & Gariépy, C. (2023). Hyperspectral imaging and chemometrics assessment of intramuscular fat in pork longissimus thoracic et lumborum primal cut. *Food Control, 145*, Article 109379.
Liu, J.-H., Sun, X., Young, J., Bachmeier, L., & Newman, D. (2018). Predicting pork loin intramuscular fat using computer vision system. *Meat Science, 143*, 18–23.
Liu, L., Ngadi, M., Prasher, S., & Gariépy, C. (2012). Objective determination of pork marbling scores using the wide line detector. *Journal of Food Engineering, 110*, 497–504.
Mahanti, N. K., Pandiselvam, R., Kothakota, A., Ishwarya, S., Chakraborty, S. K., Kumar, M., & Cozzolino, D. (2022). Emerging non-destructive imaging techniques for fruit damage detection: Image processing and analysis. *Trends in Food Science & Technology, 120*, 418–438.
Meenu, M., Kurade, C., Neelapu, B. C., Kalra, S., Ramaswamy, H. S., & Yu, Y. (2021). A concise review on food quality assessment using digital image processing. *Trends in Food Science & Technology, 118*, 106–124.
Moines, D. (1999). *Marbling standards*. National Pork Producers Council.
Muñoz, I., Gou, P., & Fulladosa, E. (2019). Computer image analysis for intramuscular fat segmentation in dry-cured ham slices using convolutional neural networks. *Food Control, 106*, 10.
Muñoz, I., Rubio-Celorio, M., Garcia-Gil, N., Guàrdia, M. D., & Fulladosa, E. (2015). Computer image analysis as a tool for classifying marbling: A case study in dry-cured ham. *Journal of Food Engineering, 166*, 148–155.
Otsu, N. (1979). A threshold selection method from gray-level histograms. *IEEE Transactions on Systems, Man and Cybernetics, 9*, 62–66.
Pu, H., Yu, J., Sun, D.-W., Wei, Q., & Wang, Z. (2023). Feature construction methods for processing and analysing spectral images and their applications in food quality inspection. *Trends in Food Science & Technology, 138*, 726–737.
Sanchez, P. D. C., Hashim, N., Shamsudin, R., & Mohd Nor, M. Z. (2020). Applications of imaging and spectroscopy techniques for non-destructive quality evaluation of potatoes and sweet potatoes: A review. *Trends in Food Science & Technology, 96*, 208–221.
Santos-Garcés, E., Muñoz, I., Gou, P., Garcia-Gil, N., & Fulladosa, E. (2014). Including estimated intramuscular fat content from computed tomography images improves prediction accuracy of dry-cured ham composition. *Meat Science, 96*, 943–947.
Sauro, J. (2011). *A practical guide to the system usability scale: Background, benchmarks & best practices*. CreateSpace Independent Publishing Platform.
Suzuki, S., & Be, K. (1985). Topological structural analysis of digitized binary images by border following. *Computer Vision Graphics Image Processing, 30*, 32–46.

Uttaro, B., Zawadski, S., Larsen, I., & Juárez, M. (2021). An image analysis approach to identification and measurement of marbling in the intact pork loin. *Meat Science, 179*, Article 108549.

Valous, N. A., Mendoza, F., & Sun, D.-W. (2010). Emerging non-contact imaging, spectroscopic and colorimetric technologies for quality evaluation and control of hams: A review. *Trends in Food Science & Technology, 21*, 26–43.

Velásquez, L., Cruz-Tirado, J., Siche, R., & Quevedo, R. (2017). An application based on the decision tree to classify the marbling of beef by hyperspectral imaging. *Meat Science, 133*, 43–50.